

Pipelined correlated minimum weight perfect matching of the surface code

Alexandru Paler^{1,2} and Austin G. Fowler³

¹*Aalto University, Espoo 02150, Finland*

²*University of Texas at Dallas, Richardson, TX 75080, USA*

³*Google Inc., Santa Barbara, 93117 CA, USA*

We describe a pipeline approach to decoding the surface code using minimum weight perfect matching, including taking into account correlations between detection events. An independent no-communication parallelizable processing stage reweights the graph according to likely correlations, followed by another no-communication parallelizable stage for high confidence matching. A later general stage finishes the matching. This is a simplification of previous correlated matching techniques which required a complex interaction between general matching and re-weighting the graph. Despite this simplification, which gives correlated matching a better chance of achieving real-time processing, we find the logical error rate practically unchanged. We validate the new algorithm on the fully fault-tolerant toric, unrotated, and rotated surface codes, all with standard depolarizing noise. We expect these techniques to be applicable to a wide range of other decoders.

I. INTRODUCTION

The surface code [1–8] is experimentally attractive as it requires only a 2D array of qubits with nearest neighbor interactions, and gate error rates of order 0.1% to achieve post-classical fault-tolerant quantum computation with fewer than 1M qubits [9]. Decoding the surface code must be done both accurately and in real time, and many algorithms have been proposed [10–15].

Realizing a scalable, accurate, real-time surface code decoder remains an open problem. To move closer to this goal, we improve the algorithm used in [14] which performs a correlated-error version of minimum weight perfect matching [16, 17].

Previously, matching was continuously performed and local reweighting of the graph, according to correlations in the underlying error model, was triggered whenever nearest neighbor detection events were matched or unmatched. Reweighting triggered erasure of the matching from current time back to the time of the reweighting, leading to significant computational overhead. This work shows that it is possible to avoid the overhead while maintaining decoding performance.

In Section II A, we describe how we extract and represent correlations in our circuits and error models. Section II B describes a round by round algorithm to use the stream of detection events to infer correlations, reweight the detection graph, and perform a partial matching of detection events. This is followed by the algorithm of [14], with no further reweighting of the detection graph. Section III describes circuit level depolarizing noise simulations of the toric, unrotated, and rotated surface codes, all with and without correlated graph reweighting.

II. METHODS

We perform correlated reweighting and an initial partial matching in a strictly round by round manner, with no backtracking or revision, and without sacrificing per-

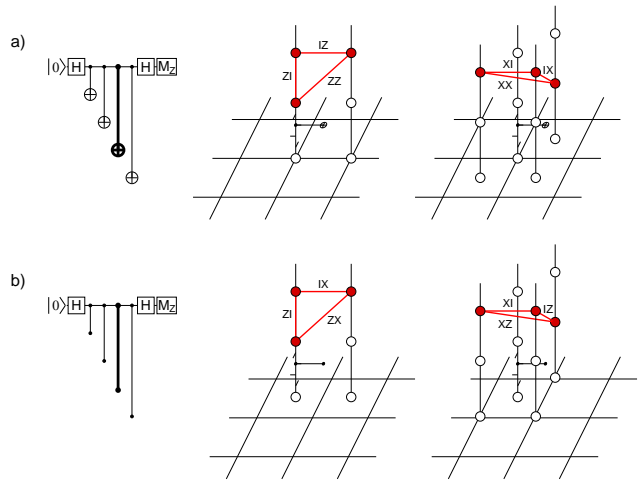


FIG. 1. Three rounds of unrotated surface code: a) X stabilizers measured on vertices; b) Z stabilizers measured on faces. Time runs horizontally in the 2D and vertically in the 3D circuits. Bolded gates suffer all possible errors with only those leading to pairs of detection events (red) shown.

formance in terms of the achieved logical error rate.

A. Correlated pre-analysis of the surface code

To illustrate how an analysis of correlations in the surface code can be performed, consider a single two-qubit gate in multiple rounds of surface code stabilizer measurement. We assume depolarizing noise, but with each of the 15 nontrivial tensor products of I, X, Y, Z potentially having a different probability. Each error on this gate can lead to anything from 0 to 4 detection events. Fig. 1 gives two examples of what can be observed.

Internally, for each gate we have a list of errors, and each error has a list of coordinates of detection events. Processing this information begins with identifying those errors that lead to single detection events. Such detec-

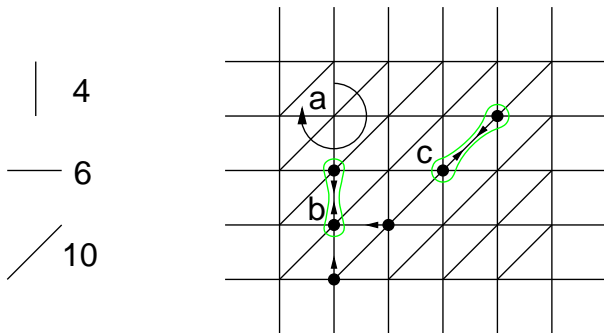


FIG. 2. Pre-matching. Example of a graph with vertical edge weights 4, horizontal edge weights 6, and diagonal edge weights 8. a) Arbitrarily chosen ordering of the edges emanating from a vertex. b) Detection event with two lowest weight neighboring detection events, namely those vertically above and below it. Given the arbitrary ordering, the one above will be chosen. Note that since the detection event above has only a single neighbor, this choice will be mutual, indicated by a green bubble. c) Detection event with two equal lowest weight diagonal neighbors, the mutual chosen pair is shown.

tion events are represented graphically by an edge to an unspecified boundary. The coordinate of the generating detection event uniquely identifies each boundary edge. A single gate may generate no or many boundary edges. Each boundary edge keeps a list of errors that generated it, and each error on this gate that generates a boundary edge is appended to the appropriate error list.

We next focus on errors that lead to pairs of detection event. If both detection events are associated with boundary edges, we skip that error for the moment, and otherwise associate an edge with the detection event coordinates. As before, such an edge keeps a list of errors that generated it, and we append each generating error to the appropriate edge’s error list.

The edges found so far form a basis, meaning all remaining errors generating 2+ detection events can be uniquely decomposed into two or more edges from this basis. Such errors are added to the error lists associated with each decomposed edge, and each copy of this error will be specially annotated with the list of decomposed lines for later processing. These decomposed lines form the basis of the correlated analysis.

When every gate in the potential computation has been analyzed in this manner, and with care this can be done without excessive duplicate processing, we will have a graph with each edge containing a list of errors, each error labeled with a generating gate, and some of these errors containing a list of decomposed edges. We now need to calculate the total probability of each edge. One could simply add up the probability of each error associated with the edge, however at higher error rates this is inaccurate and can lead to edge probabilities above 1. Instead, it is better to group the errors associated with an edge by gate, sum the probabilities of errors associ-

ated with each gate to give a list of probabilities p_i , then approximate the edge probability p_e as the probability of exactly one independent error occurring

$$p_e = \sum_i p_i \prod_{j \neq i} (1 - p_j). \quad (1)$$

Technically, the edge probability is the probability of an odd number of independent errors occurring, but the above approximation is sufficient to avoid $p_e > 1$, and achieve low logical error rates, as we shall see.

As mentioned, some of the errors associated with each edge will have a list of decomposed edges. The decomposed edges that are different from the parent are called correlated edges. Each unique correlated edge is associated with a subset of the errors associated with the parent edge. The probability of each correlated edge can be calculated using Eq. 1 with appropriately reduced p_i values. The relative probability of each correlated edge is divided by the edge probability p_e .

B. Correlated reweighting and pre-matching

The analysis in Section II A generated many edges located in space-time, each with a probability and probability of being correlated with other nearby edges. The totality of these edges is called the detection graph. Typically, it is more convenient to talk about the weight of edges rather than their probability p , with the weight $w = -\ln p$.

We present a heuristic for choosing highly likely edges in the detection graph that will be used to reweight it. We choose edges according to the following parallel pre-matching algorithm (see Fig. 2):

- For each detection event e_0 , find the set of neighboring detection events e_i with lowest weight connecting edges. If the set contains more than one, choose the one discovered first e_1 using any canonical ordering of the edges.
- For each detection event e_0 with a chosen neighboring detection event e_1 , ask e_1 if e_0 is the chosen detection event of e_1 . If yes, associate the two.

The first application of this algorithm will be called a “virtual” pre-matching, and will be used purely for detection graph reweighting.

Given a virtual pre-matching, we can use the information about correlated edges derived in Section II A to associate additional correlated probabilities p_c with nearby edges. If more than one correlated probability is associated with a single edge, we permit the algorithm to have a race condition and only keep the last written value. The final edge probability p_f is then approximated as simply $p_f = p_e + p_c$. This in turn becomes a new weight for the edge via $w = -\ln p_f$. An optional second round of pre-matching can then be performed, with the matchings kept this time and passed on to the general matching algorithm, or other decoder.

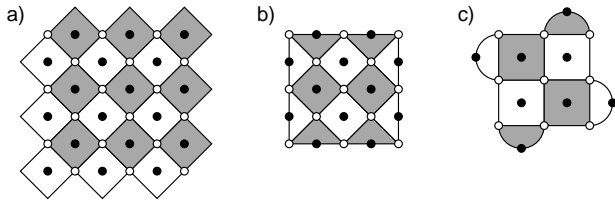


FIG. 3. Distance 3 a) toric, b) unrotated, and c) rotated surface codes. Dark plaquettes represent X stabilizers, light plaquettes represent Z stabilizers. In all 3 cases the logical X operator of interest runs from top to bottom.

III. RESULTS

To illustrate the performance of our decoding algorithm, we will simulate 3 cases, the toric, unrotated, and rotated surface codes (Fig. 3), each with and without correlated graph re-weighting. Simulation results can be found in Figs. 4–6.

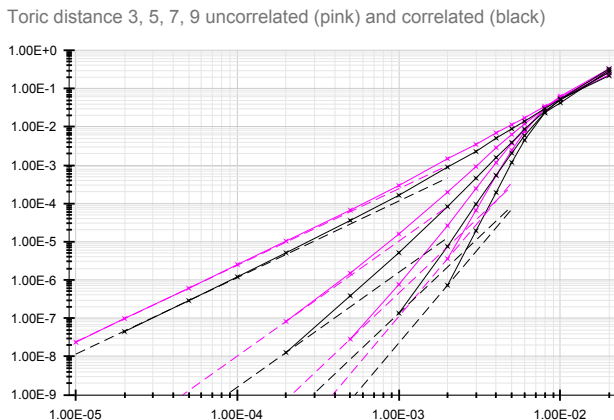


FIG. 4. Toric uncorrelated (pink) and correlated (black) distance 3–9 simulations. Dashed lines show p^2 , p^3 , p^4 and p^5 lines respectively, the asymptotic slope of each line. The fact that the data curves are much steeper than the asymptotic curves for high distances and high gate error rates shows that logical errors are suppressed at even higher powers than these in this regime.

To the best of our knowledge, this is the first time these 3 commonly studied cases have been simulated with a single framework with results gathered in one place for comparison. We will use standard equal gate duration 8-step CNOT-based circuits as shown in Fig. 1a, with all gates suffering standard depolarizing noise of equal probability p . Explicitly, initialization and measurement prepare and measure the wrong states with probability p , single-qubit gates including the identity suffer X, Y, Z errors each with probability $p/3$, and CNOT gates suffer all 15 non-trivial tensor products of I, X, Y, Z each with probability $p/15$.

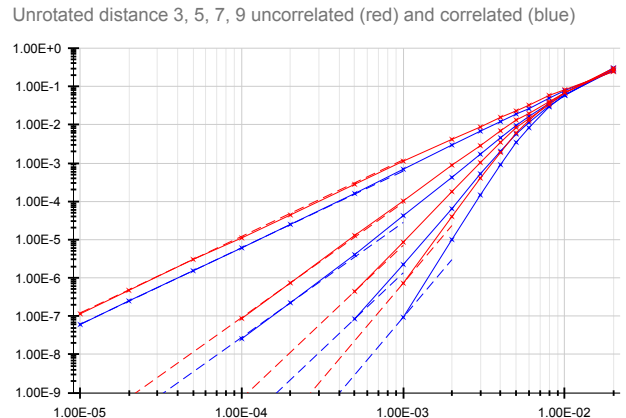


FIG. 5. Unrotated uncorrelated (red) and correlated (blue) distance 3–9 simulations.

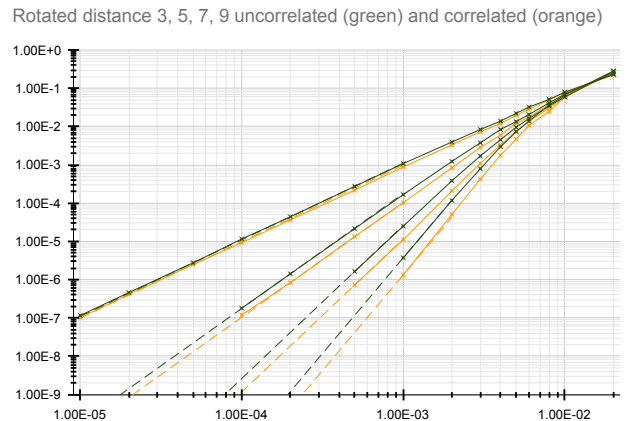


FIG. 6. Rotated uncorrelated (green) and correlated (orange) distance 3–9 simulations.

We focus on the logical X failure rate per round, and measure this by simulating a sufficiently large number of rounds N such that the final probability of logical error is around 10%, then equate this with the probability of obtaining an odd number of logical errors in N and back out the failure rate per round using a sum of binomial terms.

The simulations of Fig. 5 are indistinguishable from those reported in [14], with the distance 3 logical X error in both cases just below 10^{-7} at a physical error p of 10^{-5} , and the distance 9 logical X error also in both cases just below 10^{-7} at a physical error p of 10^{-3} .

IV. CONCLUSION

A pipeline approach is a step towards real-time decoding of the surface code. We presented a method that operates on the stream of detection events and processes

the data in a sequence stages implemented in a parallelizable manner that requires no communication.

The stages of the pipeline are: reweighting, pre-matching and full-matching. The functionality of the first two stages is based on a novel analysis of correlated errors. The correlated analysis is decoder agnostic, and the graph re-weighting highly hardware compatible. One can imagine measurements from a quantum computer streaming through dedicated hardware to generate a re-weighted graph with optional partial matching that is then passed on to another decoder of the users choice.

Simulation results for the toric, rotated and unrotated surface code support the feasibility of the pipeline approach. Future work will focus on extending our results to other decoder types.

ACKNOWLEDGMENTS

AP was supported by Google Faculty Research Awards and a Fulbright Senior Researcher Fellowship.

-
- [1] S. B. Bravyi and A. Y. Kitaev, Quantum codes on a lattice with boundary, *quant-ph/9811052* (1998).
- [2] E. Dennis, A. Kitaev, A. Landahl, and J. Preskill, Topological quantum memory, *J. Math. Phys.* **43**, 4452 (2002), *quant-ph/0110143*.
- [3] R. Raussendorf and J. Harrington, Fault-tolerant quantum computation with high threshold in two dimensions, *Phys. Rev. Lett.* **98**, 190504 (2007), *quant-ph/0610082*.
- [4] R. Raussendorf, J. Harrington, and K. Goyal, Topological fault-tolerance in cluster state quantum computation, *New J. Phys.* **9**, 199 (2007), *quant-ph/0703143*.
- [5] A. G. Fowler, M. Mariantoni, J. M. Martinis, and A. N. Cleland, Surface codes: Towards practical large-scale quantum computation, *Phys. Rev. A* **86**, 032324 (2012), *arXiv:1208.0928*.
- [6] A. G. Fowler and C. Gidney, Low overhead quantum computation using lattice surgery, *arXiv:1808.06709* (2018).
- [7] D. Litinski, A game of surface codes: Large-scale quantum computing with lattice surgery, *Quantum* **3**, 128 (2019), *arXiv:1808.02892*.
- [8] C. Gidney and A. G. Fowler, Flexible layout of surface code computations using autoccz states, *arXiv:1905.08916* (2019).
- [9] I. D. Kivlichan, C. Gidney, D. W. Berry, N. Wiebe, J. McClean, W. Sun, Z. Jiang, N. Rubin, A. G. Fowler, A. Aspuru-Guzik, H. Neven, and R. Babbush, Improved fault-tolerant quantum simulation of condensed-phase correlated electrons via trotterization, *Quantum* **4**, 296 (2020), *arXiv:1902.10673*.
- [10] R. S. Andrist, H. Bombin, H. G. Katzgraber, and M. A. Martin-Delgado, Optimal error correction in topological subsystem codes, *Phys. Rev. A* **85**, 050302R (2012), *arXiv:1204.1838*.
- [11] G. Duclos-Cianci and D. Poulin, Fault-tolerant renormalization group decoder for Abelian topological codes, *Quant. Inf. Comput.* **14**, 0721 (2014), *arXiv:1304.6100*.
- [12] A. Hutter, J. R. Wootton, and D. Loss, An efficient Markov chain Monte Carlo algorithm for the surface code, *Phys. Rev. A* **89**, 022326 (2014), *arXiv:1302.2669*.
- [13] J. R. Wootton, A simple decoder for topological codes, *Phys. Rev. A* **88**, 062312 (2013), *arXiv:1310.2393*.
- [14] A. G. Fowler, Optimal complexity correction of correlated errors in the surface code, *arXiv:1310.0863* (2013).
- [15] P. Baireuther, M. D. Caio, B. Criger, C. W. J. Beenakker, and T. E. O'Brien, Neural network decoder for topological color codes with circuit level noise, *New J. Phys.* **21**, 013003 (2019), *arXiv:1804.02926*.
- [16] J. Edmonds, Paths, trees and flowers, *Canad. J. Math.* **17**, 449 (1965).
- [17] J. Edmonds, Maximum matching and a polyhedron with 0,1-vertices, *J. Res. Nat. Bur. Standards* **69B**, 125 (1965).

APPENDIX: PRE-MATCHING

This section describes the method and implementation of pre-matching and how it is used during the analysis of correlated errors. To this end an error detection graph like the one from Fig. 7 is used. Each graph vertex has an associated 3D coordinate of the type (t, i, j) where (i, j) are coordinates of the physical qubit that generated the detection event, and t is an integer indicating time. Later detection events have higher values of t .

Pre-matching uses only local information without explicitly including a method for achieving a global optimum low weight matching. It is a greedy algorithm that assigns three types of states to a detection event: zero-prematched (ZP), half-prematched (HP) and fully-prematched (FP). Two examples are presented in Figs. 8 and 9. The temporal ordering of the detection events plays a role in how states are assigned and transformed. The PMC of all the events is processed in the following order: a) increasing time t ; b) increasing i -coordinate and c) increasing j -coordinate.

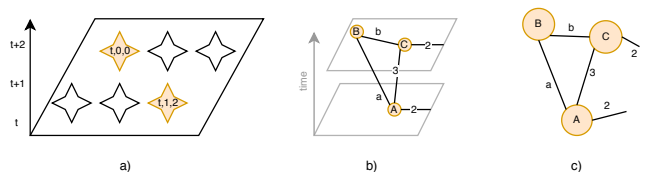


FIG. 7. Prematching: a) Detection events have 3D coordinates, and are processed in the order of their time, row and column coordinates. For example, the first event to process is $(1,0,0)$ and the second is $(1,1,2)$. b) A graph of three detection events (A, B, C) is built and the weights of the edges are computed. In this example, only for the events A and C we consider the edges to the boundary of the code patch. c) The graph after eliminating the time layers visualization.

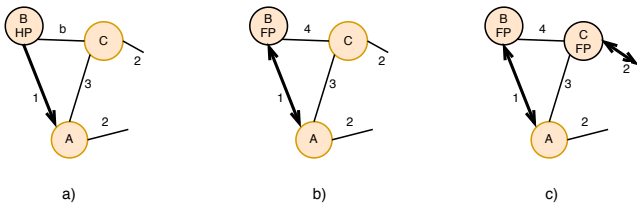


FIG. 8. Advancing the state of the vertices. All vertices start in ZP (not illustrated) and the pre-match order is A, B, C. Example obtained by replacing $a=1$ and $b=4$ in Fig. 7c.: a) The lowest weight edge is the one connecting A to B, such that B is marked as half prematched HP stores a reference to A; b) After pre-matching B, the lowest weight edge points to A, and the state of B is updated to full prematched FP; c) The lowest edge weight of C is the one connecting to the boundary, and C is automatically fully prematched.

a. Pre-matching condition (PMC)

We use the symbol \leftrightarrow to indicate that two events A and B are FP, fully prematched. We call *PMC* the event pre-match condition that establishes one direction of the prematching, either \rightarrow or \leftarrow . Two events A and B are fully prematched, the $A\leftrightarrow B$ relation exists, if $A\rightarrow B$ and $A\leftarrow B$. We use both directions of the arrows (\rightarrow and \leftarrow) because we assume a temporal ordering between the detection events A and B (cf. Table I). If the PMC is checked from A towards the future B then $A\rightarrow B$, otherwise if from a later B to a sooner A then $A\leftarrow B$.

A strict PMC can be formulated as $A\rightarrow B$ if B is the only neighbor of A in the error detection 3D graph. The condition guarantees that the prematched events are also valid matchings from the perspective of minimum weight perfect matching. However, at high physical error rates, the strict PMC is very seldom fulfilled, because detection events are more probable and have more than one neighbor in the graph. We introduce a relaxed PMC condition, such that more events are prematched without offering any guarantees that these form minimum weight matches.

Initially, all detection events are in the state ZP. Half-pre-matching is performed towards the future, meaning that if the event B is later than A, and $A\rightarrow B$ then B will be in the HP state (if it was ZP) and will store a reference to A (e.g. Fig. 8a). When it is the turn of B to be analysed for prematching, if $C\leftarrow B$ and C is the same as the stored reference to A, then the state of B is transformed from HP to FP.

b. Pre-matching with the boundary

The goal of pre-matching is to pair detection events and avoid where possible matching with the boundary (e.g. Fig. 9c). pre-matching with the boundary is avoided as, in general, locally matching with the boundary seems to be the lowest weight choice, but when considering the

		coord(B) < coord(A)			coord(A) < coord(B)			
A	B			B	A			E
	ZP	HP	FP		ZP	HP	FP	
ZP	ZP	E	ZP	ZP	HP	ZP _A	E	
HP	FP/ZP	E	E/ZP	HP	E/ZP	E/ZP _{A,B}	E	
FP	E	E	E	FP	E	E	E	

TABLE I. The state transformation rules when performing pre-matching starting from detection event A. Detection event B has the lowest weight from the neighborhood of A and is fulfilling the PMC. Depending on the coordinate of B, returned by the function $coord$, one of the two state transition tables is used. When not indicated by a subscript, the state of the latest (bold) detection event is updated.

global sum of the weights this is often not the case.

Matching with the boundary is allowed whenever a detection event is processed and no other detection event in its neighborhood has the state FP (valid state from the past, cf. Table I) or HP (valid state in the future, cf. Table I). Considering two neighboring detection events A and B where both could be connected to the boundary we assume that such a decision will not result in a low weight global matching. For small distances, the ratio of events close to the boundary is higher than for larger distances. However, we consider that decoding should perform well for large distances and that our heuristic will result in *more realistic looking* matches.

c. Vertex state updates

The method updates the states of the detection event vertices. If an event's state is ZP and it can be connected to the boundary, then the state is automatically updated to FP and the next detection event is considered. Otherwise, the state transformation procedure from the following paragraphs is applied.

The state transitions from in Table I are independent of the PMC. As a general rule:

1. before processing a detection event the only valid states are ZP and HP (if it has been half-matched in the past);
2. after processing an PMC, the only valid states will be ZP and FP.

The pre-match algorithm raises an error E each time it was implemented in an inconsistent or incorrect manner. This makes pre-matching a candidate for parallelisation and offers the rules for enforcing and checking data consistency when multiple processes are updating in parallel the detection event states.

pre-matching updates the state of the detection events with coordinates from the present and future, greater or equal to $coord(A)$. The pre-matching procedure does not update states of detection events from the past. This functionality is to make pre-matching more compatible with stream processing.

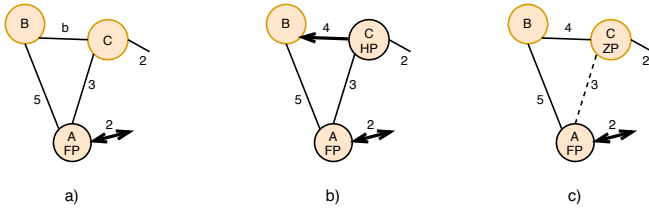


FIG. 9. Reverting the state of the vertices. All vertices start in ZP (not illustrated) and the pre-match order is A, B, C. Example obtained by replacing $a=5$ and $b=4$ in Fig. 7c.: a) The lowest weight edge is connecting to the boundary, and A is automatically fully prematched. b) When pre-matching B, the lowest weight edge is towards C which is half prematched and will store a reference to B. c) Because A is FP and in the neighborhood of C, the lowest weight edge (2) is not considered and the next best option is pointing towards A (3), such that C cannot be prematched and its state is reset to ZP.

Considering that A is the detection event that is processed, and that the PMC function returns B, there are two possibilities:

- B has a coordinate lower than A;
- B has a coordinate higher than A.

For the first situation, $coord(B) < coord(A)$ (cf. Fig. 9c where C is processed and $coord(A) < coord(C)$), if B has state HP, then it is always an error, because B should have been already processed and its state is not valid. If the state of A is FP, this is impossible and always an error, because A is only now being processed. This leaves only four non-error transitions:

1. If A is ZP and B is ZP, then the state of A is not changed, because B is in the past.
2. If A is half-prematched HP and B is ZP, if the backwards reference from A points to B then both PMC directions are fulfilled and B is fully prematched and its state transitions to FP.
3. If the reference does not point to B, then the state of A is reset to ZP.
4. If A is HP but the B from the past is already fully prematched, then it is an obvious error if the reference from A points to B, and otherwise the state of A is reset to ZP.

In the second situation, $coord(A) < coord(B)$, it is always an error if A is FP. Also it is not possible for B to be FP, because it is in the future and could not have been processed by now (cf. Fig. 8a where A is processed). This leaves four possible configurations:

1. If both A and B are ZP, then the state of B is changed to HP and B will store a reference to A.
2. If A is HP and the future B is still ZP, it means that the backwards PMC for A is not fulfilled and the state of A is reset to ZP.
3. If B is HP and its reference points to A, it is definitely an error, because A is only now being processed and could have not changed the state of B to HP. Otherwise, if B is HP and A is ZP, then the state of A is kept ZP and the state of B is reset to ZP (this is a strict rule, the state of B could have been kept HP and be processed only later).
4. If B is HP and A is HP, the states of both A and B is reset to ZP.